Romanian Reports in Physics, Vol. 65, No. 3, P. 943–953, 2013

Dedicated to Professor Valentin I. Vlad's 70th Anniversary

LASER EMISSION IN DIODE-PUMPED Nd:YAG SINGLE-CRYSTAL WAVEGUIDES REALIZED BY DIRECT FEMTOSECOND-LASER WRITING TECHNIQUE

G. SALAMU[1], F. VOICU[1], N. PAVEL[1], T. DASCALU[1], F. JIPA[2], M. ZAMFIRESCU[2]

National Institute for Laser, Plasma and Radiation Physics, Bucharest 077125, Romania
[1]Laboratory of Solid-State Quantum Electronics
[2]Laser Department, Solid-State Laser Laboratory
Email: gabriela.salamu@inflpr.ro, nicolaie.pavel@inflpr.ro

Received May 22, 2013

Abstract. Buried waveguides have been realized in a 0.7 at.% Nd:YAG single crystal using the direct-writing technique with a femtosecond laser. Efficient laser emission at 1.06 and 1.32 μm is demonstrated and laser action at 0.94 μm is obtained using the pump with fiber-coupled diode laser at 807 nm, the first demonstration of such devices.

Key words: lasers, solid-state, lasers, diode-pumped, lasers, neodymium, pumping, optical waveguides.

1. INTRODUCTION

The waveguide lasers [1] are of special interest in optoelectronics due to their compact dimensions, low threshold of emission and good output performances. Such optical devices can be fabricated in an existing host by various methods, like thermal ion indiffusion [2], ion exchange [3] or proton exchange [4], proton or ion beam irradiation [5, 6], or by direct writing with a femtosecond (fs) laser [7-9]. Using the direct fs-laser writing technique, two types of tracks can be realized in a host, depending on the material properties and on the fs-laser characteristics. The first kind is specific to glasses and $LiNbO_3$ and consists of a single line; this method provides a track that is used itself for light propagation. The second type of writing damages the material inside the inscribed track and causes a stress induced refractive index change in the adjacent region; in this case the light is guided in between two such tracks.

Double-wall waveguides were obtained in various laser media, such as Nd:YAG [9-11], Nd-vanadates [12, 13], Yb:YAG [14, 15], Nd:$Gd_3Ga_5O_{12}$ [16, 17], or Pr:$YLiF_4$ (Pr:YLF) [18]. The pump with a Ti:sapphire laser was employed to

demonstrate continuous-wave (cw) efficient laser emission around 1 μm in these waveguides. Output power of ~80 mW at 1.06 μm for ~200 mW of incident pump power at 748 nm and slope efficiency (η_s) of 0.60 was obtained from a Nd:YAG ceramics waveguide [9], while the pump with 2.25 W of power at 808 nm yielded 1.3 W output power at 1.06 μm with slope η_s= 0.54 from a Nd:YAG single-crystal waveguide [11]. Maximum output power of 9.5 mW at 1.064 μm for 39 mW absorbed pump power at 808 nm and slope efficiency with respect to the absorbed pump power (η_{sa}) of 0.39 was obtained from a Nd:YVO_4 waveguide [12]. A Nd:$GdVO_4$ waveguide delivered 256 mW cw output power at 1.064 μm for 569 mW absorbed pump power with slope η_{sa}~ 0.70 [13]. An Yb:YAG single-crystal waveguide yielded 0.8 W at 1.03 μm for 1.2 W of pump power at 941 nm with slope η_s= 0.75 [14]. Double-wall waveguides were also fabricated in a multifunctional Nd:YVO_4-KTP hybrid system [19] or in a KTP nonlinear crystal for broadband second harmonic generation [20].

Inscribing many tracks around the perimeter of a desired configuration is a method used to obtain depressed cladding waveguides. These devices are buried structures consisting of a low-index tubular cladding that surrounds a non-modified core of the medium [8]. Such a waveguide has low propagation loss and possess flexibility for different shapes and size, thus enabling good coupling to the waveguide of the pump beam delivered through a fiber. The pump with Ti: sapphire of a Nd:YAG circular cladding waveguide yielded 181 mW cw output power at 1.06 μm [21], and ~93 mW output power at 1.98 μm was obtained from such a Tm:YAG waveguide [22]. Buried cladding waveguides of various shapes were also realized in other laser media, such as Pr:YLF [23], Nd: $La_3Ga_5SiO_{14}$ [24] or the self-frequency-doubling Nd:$YAl_3(BO_3)_4$ crystal [25].

The output performances of these fs-laser written waveguide lasers were investigated mainly under the pump with Ti:sapphire laser; this assures good coupling of the pump beam in the waveguide as well as high absorption efficiency, but the laser device can not be made compact. Recently, cw output power of 180 mW at 1.06 μm for the pump with a fiber-coupled diode-laser emitting about 1 W at 808 nm was obtained from a nearly circular cladding waveguide that was inscribed in a Nd:YAG crystal [26]. On the other hand, the laser emission in these Nd-based waveguides was made in principal at 1.06 μm. To date, simultaneous emission at 1064 and 1342 nm was reported in a fs-laser written Nd:YVO_4 waveguide, however with low efficiency at 1342 nm; thus, the slope efficiency at 1342 nm was η_{sa}~ 1.7% and the maximum output power amounted at 5 mW [27].

In this paper we report on realization of double-wall type and depressed cladding waveguides in a Nd:YAG single crystal using the direct writing technique with a fs laser. Furthermore, we demonstrate efficient laser emission on the four level $^4F_{3/2}\rightarrow{}^4I_{11/2}$ transition at 1.06 μm and the 1.32-μm $^4F_{3/2}\rightarrow{}^4I_{13/2}$ line, as well as laser action on the quasi-three-level $^4F_{3/2}\rightarrow{}^4I_{9/2}$ transition at 946 nm, under the

pump with a fiber-coupled diode laser at 807 nm. Laser pulses at 1.06 μm with energy (E_p) of 1.8 mJ for 9.1 mJ energy of the pump pulse (E_{pump}) were obtained from a circular, 120 μm diameter depressed cladding waveguide; the slope efficiency was η_s= 0.22. This configuration outputted 0.54 W cw output power at 1.06 μm under the pump with 3.8 W power; the slope was η_s= 0.17. For operation at 1.32 μm the laser pulse energy reached 0.40 mJ and slope amounted at η_s= 0.10. Laser emission at 946 nm with E_p = 0.12 mJ was obtained from the same waveguide. Results on other depressed cladding and two-wall type waveguides are discussed. To the best author knowledge this is the first demonstrations of laser emission at 0.94 and 1.32 μm from fs-laser written waveguides in Nd:YAG, as well as one of the first reports on laser emission in such waveguides under the pump with fiber-coupled diode laser.

2. RESULTS AND DISCUSSION

2.1. WAVEGUIDE FABRICATION AND CHARACTERIZATION

A chirped pulsed amplified fs-laser system (Clark CPA-2101) that yielded pulses with 200 fs duration and energy up to 1 mJ at 775 nm at a repetition rate of 2 kHz was used to write the tracks; a sketch of the experimental set-up is shown in Fig. 1. The laser medium was a 0.7-at.% Nd:YAG single crystal (length ℓ= 5.4 mm, thickness t = 3.0 mm, width w = 6.0 mm). The crystal was placed on a motorized translation stage that allowed controllable movement on all directions. The energy of the fs-laser beam incident on Nd:YAG was varied by a combination of half-wave plate (λ/2), a polarizer (P), and a neutral filter (F). A 20× microscope objective with a numerical aperture (NA) of 0.40 was used to focus the fs-laser beam to a focus (in air) of ~7 μm diameter and 65 μm confocal parameter. The tracks were inscribed on Ox direction, using a 50 μm/s speed of the translation stage; the writing process was monitored with a video camera that was positioned perpendicular to the Ozy surface of Nd:YAG.

Tracks were written on and below the Nd:YAG top surface. We mention that from preliminary attempts it was concluded that the threshold energy of the fs-laser pulse that realizes modifications on Nd:YAG surface was 2.7 μJ. Then, the fs-laser pulse energy was increased at 3.3 μJ and pair of tracks with 40 μm distance between were made on Nd:YAG surface, as shown in Fig. 2a. For the tracks inscribed below the Nd:YAG surface the fs-laser pulse energy was increased even more, at 3.9 μJ. Figure 2b presents a traditional two-wall structure (denoted by WG-1); the size of such a geometry on direction Oz was increased by writing six lines, as shown in Fig. 2c (WG-2). Tubular depressed claddings of square, rectangular, circular or ellipsoidal shapes were also realized by inscribing equally

spaced (at 4 or 10 μm distance between) tracks around each geometry perimeter. Each structure was centered at a depth h = 250 μm under the Nd:YAG surface. A rectangular shape (cross section with B = 40 μm and C = 50 μm) is shown in Fig. 2d (this structure will be denoted by DWG-3). Other two round geometries, the first with diameter D = 80 μm (DWG-4) and the second elliptical with horizontal axis E = 120 μm and vertical axis F = 165 μm (DWG-5), are shown in Fig. 2e and Fig. 2f, respectively. After the writing process, the end faces of the Nd:YAG were polished, this process reducing the crystal length ℓ at 5.0 mm.

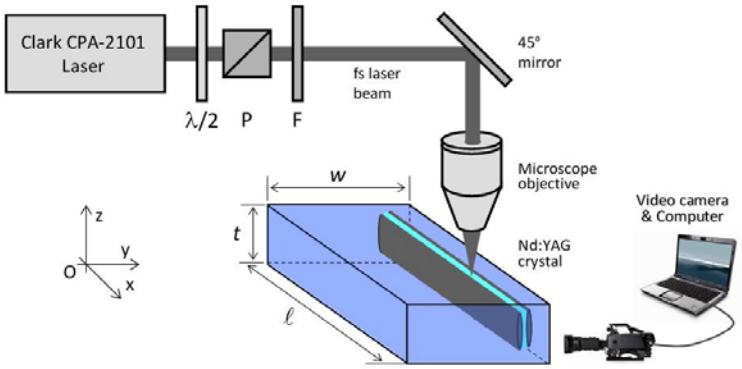

Fig. 1 – The experimental set-up used for writing of tracks in Nd:YAG with a fs laser is presented. λ/2 – half-wave plate, P – polarizer, F – neutral filter; w – width, ℓ – length, t – thickness.

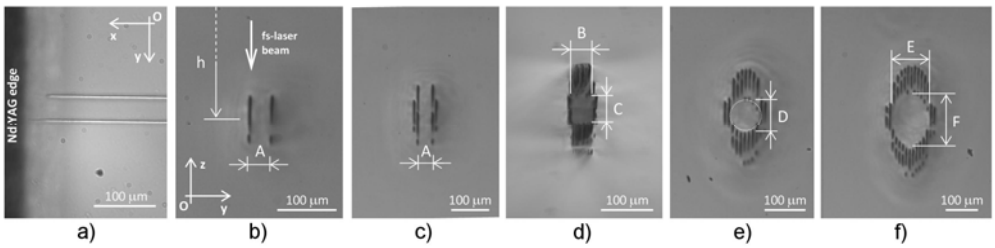

Fig. 2 – Microscope photos of: a) two lines inscribed on the Nd:YAG surface, and of various structures realized inside the Nd:YAG crystal; b) two tracks distance A= 40 μm; c) six tracks for a two-wall structure with increased dimension on direction Oz. Depressed cladding structures with: d) rectangular (B = 40 μm, C = 50 μm); e) circular (D = 80 μm) and f) elliptical (E = 120 μm, F = 165 μm) shapes.

Waveguiding can be obtained between two parallel tracks (WG-1 and WG-2), or in the centre of the tubular depressed structures (DWG-3, DWG-4 and DWG-5). In order to evaluate the propagation losses of each configuration, a HeNe laser beam was coupled into every structure and the power of the transmitted light was measured. The HeNe beam was polarized to the long axis of the cross section of

the written tracks (axis O*z* in Fig. 1). These experiments concluded that propagation losses at 632.8 nm were between 1.1 and 1.4 dB/cm for the two-wall waveguides, in the range of 1.3 to 1.6 dB/cm for the circular cladding waveguides, and higher, *i.e.* 2.2 dB/cm, for the rectangular-shape cladding waveguide. These numbers are bigger than those reported for a two-wall waveguide that was written in a Nd:YAG ceramics medium (0.6 dB/cm at 748 nm) [9], but comparable with losses of the two-wall waveguides inscribed in Nd:YAG single-crystals (1.1 dB/cm at 632.8 nm or 1.6 dB at 1063 nm) [10, 11] or with losses of the depressed cladding waveguides realized in Nd:YAG ceramics (0.8 to 1.4 dB/cm at 632.8 nm) [22].

2.2. LASER EMISSION. RESULTS AND DISCUSSION

The optical pumping was made with a fiber-coupled diode laser (LIMO Co., Germany) with wavelength at 807 nm (λ_p) and that was operated in quasi-cw mode (pump pulse duration of 1 ms at 5 Hz), as well as in cw regime. The fiber end (with diameter of 100 μm and NA= 0.22) was imaged into the Nd:YAG medium using a collimating lens of 50 mm focal length and a lens of 30 mm focal length for focusing. The optical resonator consisted of a plan high-reflectivity mirror (HRM) that was coated HR (reflectivity, $R > 0.998$) at the laser wavelength of 946 nm, 1.06 or 1.32 μm (λ_{em}) and with high transmission, HT (transmission, $T > 0.98$) at λ_p, and plane or concave output coupling mirrors (OCM) of various T at λ_{em}. The resonator mirrors were positioned close of the uncoated Nd:YAG crystal, which was placed on an aluminum plate without any cooling.

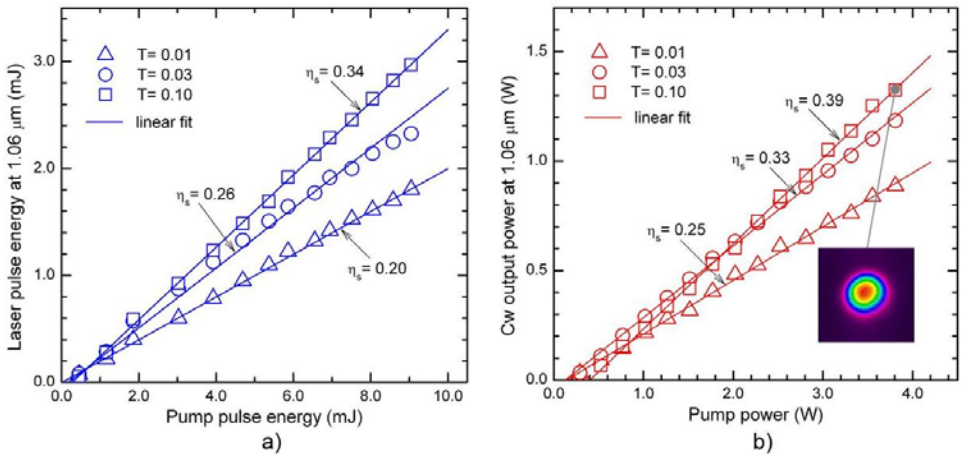

Fig. 3 – Performances of laser emission at 1.06 μm obtained from bulk Nd:YAG under the pump with diode laser in: a) quasi-cw; b) cw regimes, plane-plane resonator. Inset of Fig. 3b shows the 2D profile of the laser beam at the indicated point, where T – transmission of the output mirror.

Figure 3 presents the laser emission performances at λ_{em}= 1.06 μm (*i.e.* the four-level $^4F_{3/2} \rightarrow {}^4I_{11/2}$ transition) obtained from bulk Nd:YAG. In quasi-cw pumping regime, the laser delivered pulses with energy E_p= 2.97 mJ for the pump with pulses of energy E_{pump} = 9.1 mJ, corresponding to an overall optical-to-optical efficiency, η_o of ~0.33; the slope efficiency was η_s= 0.34 (Fig. 3a). The resonator was plane-plane with OCM of transmission T = 0.10 at λ_{em}. Absorption efficiency of the pump radiation was η_a= 0.70 and therefore the optical efficiency and slope efficiency with respect to the absorbed pump energy amounted to η_{oa}~ 0.47 and η_{sa}~ 0.49, respectively. In cw operation the pump power was kept below 4.0 W, due to thermal effects in Nd:YAG. The output power reached 1.3 W (η_o~ 0.34) with slope η_s= 0.39, as shown in Fig. 3b. Absorption efficiency was η_a= 0.82 and therefore efficiencies η_{oa} and η_s for cw operation in bulk Nd:YAG were 0.42 and 0.48, respectively. It is worthwhile to mention that similar data were recorded in both quasi-cw and cw pumping regimes when the flat OCM was replaced with concave mirrors of 50 or 200 mm radius and the same transmission T = 0.10.

Laser emission at 1.06 μm was obtained in all the waveguides presented previously. Figure 4 shows images of the transmitted pump light at the Nd:YAG exit surface. For the two-wall type waveguides a polarizer was inserted between the collimating and the focusing lens in order to obtain a polarized pump beam.

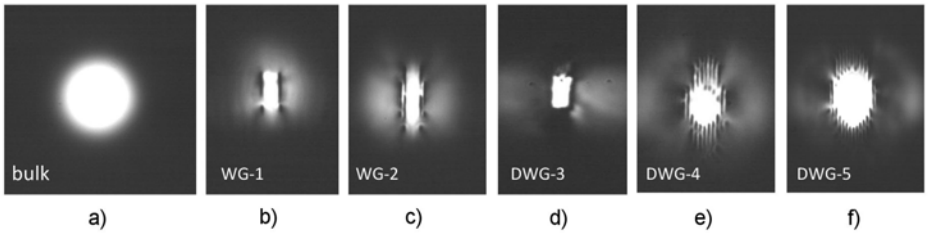

Fig. 4 – Images of the pump light at the ZY surface of Nd:YAG recorded from: a) bulk Nd:YAG, the two-wall type waveguides; b) WG-1; c) WG-2, and the depressed cladding waveguides; d) DWG-3; e) DWG-4 and f) DWG-5.

Figure 5 shows the laser emission characteristics recorded from the depressed buried waveguides (randomly polarized pump beam). The DWG-5 device emitted laser pulses with E_p = 1.4 mJ (optical efficiency η_o~0.155) when OCM was flat with T = 0.10; slope efficiency and threshold of emission (E_{th}) were η_s= 0.22 and ~2.5 mJ, respectively (Fig. 5a). On the other hand, E_{th} reduced at 0.8 mJ and E_p increased at 1.8 mJ (η_o~0.20) with a concave OCM of 200 mm radius and T = 0.10. Lower performances were measured from the other two waveguides, as shown in Fig. 5b. Thus, maximum pulse energy was E_p = 0.7 mJ and slope η_s amounted to 0.14 for DWG-4, while E_p and η_s were 0.4 mJ and 0.09 for the DWG-3 waveguide.

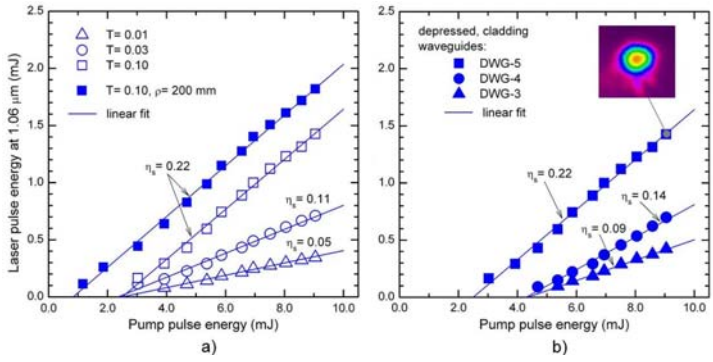

Fig. 5 – Laser pulse energy at 1.06 μm *versus* pump pulse energy for: a) the depressed, cladding waveguide DWG-5, OCM of various transmission T; b) the depressed cladding waveguides used in the experiments, plane-plane resonator with OCM of $T = 0.10$. Inset of Fig. 5b shows the 2D projection of the laser beam at the indicated point.

Comparison between laser performances obtained in bulk and in the waveguide is difficult, because various parameters, such as the fraction of the pump power that is coupled into the waveguide, the waveguide losses or absorption efficiency of the pump radiation in waveguide, can not be determined exactly. Nevertheless, using an integral overlap between the pump beam distribution and the waveguide input surface we evaluate the pump beam coupling efficiency to η_c~0.90 for DWG-5, and to ~0.50 and ~0.30 for DWG-4 and DWG-3, respectively. Therefore, the slope efficiency with respect to the coupled energy of the pump pulse was in the range of 0.24 to 0.30 for all the depressed cladding waveguides. As shown in Fig. 6, the slope η_s was 0.24 for WG-2 and 0.28 for WG-1. These values are higher than those recorded from the depressed cladding waveguides and were related to lower losses of the two-wall type waveguides.

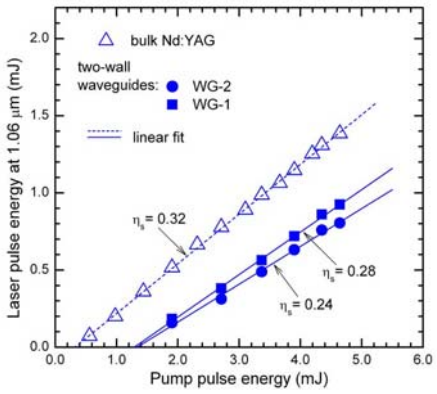

Fig. 6 – Energy of the laser pulse at 1.06 μm obtained from the two-wall waveguides (linear polarized beam), plane-plane resonator, OCM with $T = 0.10$. Experimental data for laser emission in bulk Nd:YAG under the pump with polarized beam are given.

Characteristics of cw emission at 1.06 μm are shown in Fig. 7. The DWG-5 waveguide delivered 0.39 W maximum output power with slope $\eta_s = 0.11$ (plane-plane resonator, OCM with $T = 0.10$). Furthermore, the two-wall waveguide WG-1 yielded 0.49 W cw output power (linearly-polarized beam) with optical efficiency $\eta_o \sim 0.15$. It was observed that the output power obtained from WG-2 saturated for pump powers beyond 2.2 W, while the other depressed cladding waveguides operated only near threshold. Inset of Fig. 7 presents near field distribution of the cw laser beams at the indicated points. While for operation in bulk Nd:YAG the laser beam profile (shown in Fig. 3b) has a symmetrical shape and was stable, the laser beams yielded from the waveguides showed power and distribution variations in time. Furthermore, such behavior was not observed under quasi-cw pumping (typical laser distribution was shown in Fig. 5b). These variations (in cw regime) were attributed to thermal effects in Nd:YAG that could expand the crystal and moves the waveguide out of the pump beam focusing position. Nevertheless, the output power recovered after the optical pump was stopped and the laser was started again. Therefore, cooling of the waveguides is necessary for stable laser operation in cw operation mode.

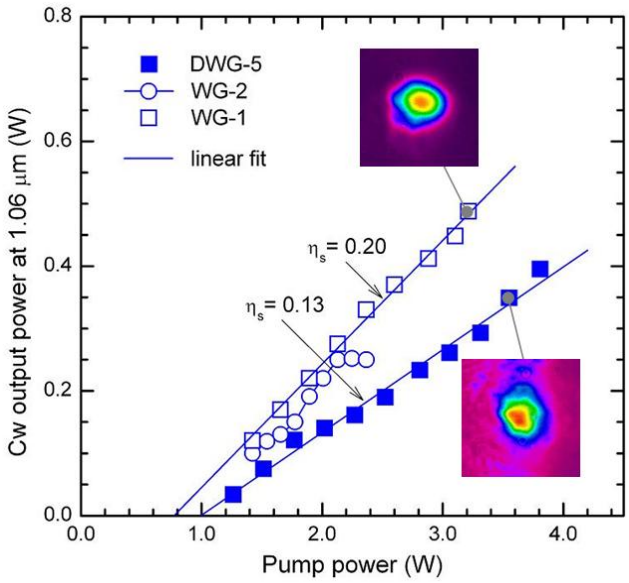

Fig. 7 – Cw output power 1.06 μm obtained from waveguides WG-1 and WG-2 (linearly polarized beams) and DWG-5 (randomly polarized beam), plane-plane resonator, OCM with $T = 0.10$. Insets show the laser beam distributions at the indicated points.

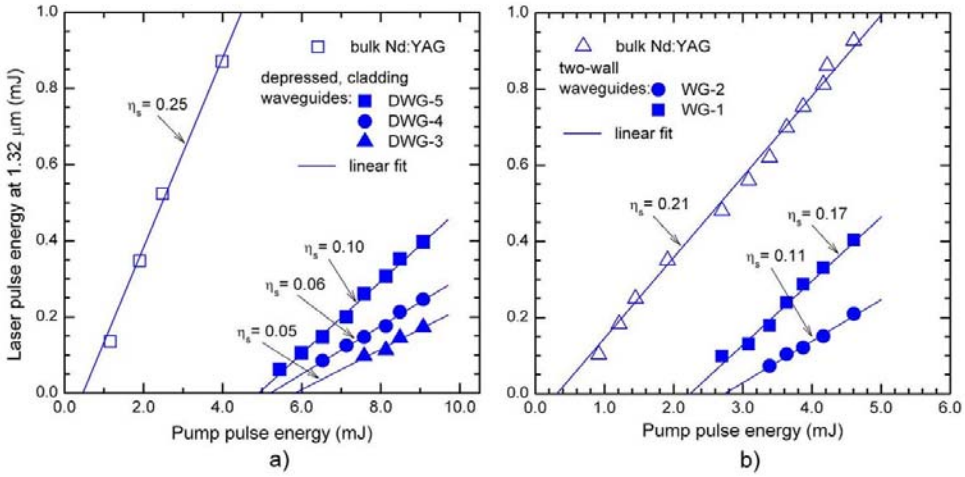

Fig. 8 – Laser pulse energy at 1.32 μm obtained from a) the depressed, cladding waveguides (randomly polarized beams) and from b) the two-wall type waveguides (linearly polarized beams), plane-plane resonator, OCM with $T = 0.03$. Comparative data for operation in bulk Nd:YAG are given.

In order to obtain laser emission at 1.32 μm (on the four-level $^4F_{3/2} \rightarrow {}^4I_{13/2}$ transition) the optical resonator was equipped with an HRM at this wavelength, while the OCM has a specified T at 1.32 μm, but presented also dielectric coating with HT (T> 0.95) at 1.06 μm in order to suppress laser emission at this high-gain line. Figure 8 shows the output characteristics at 1.32 μm recorded in quasi-cw regime with an OCM of $T = 0.03$. The DWG-5 waveguide yielded laser pulses with $E_p = 0.4$ mJ ($E_{pump}= 9.1$ mJ), while the slope efficiency was $\eta_s \sim 0.10$ (Fig. 8a). The pulse energy E_p decreased at 0.25 mJ and slope was $\eta_s= 0.06$ for the cylindrical DWG-4 waveguide, while laser pulses with energy $E_p = 0.17$ mJ at slope $\eta_s= 0.05$ were available from DWG-3. The two-wall WG-1 waveguide showed good performances, emitting laser pulses with $E_p = 0.4$ mJ for incident polarized beam of energy $E_{pump}= 4.6$ mJ; the slope efficiency was $\eta_s \sim 0.17$ (Fig. 8b).

Cw operation at 1.32 μm was also obtained, although of low performances. Thus, WG-1 yielded 0.11 W power for the pump power of 3.2 W; the slope efficiency was $\eta_s= 0.05$. The other waveguides delivered much lower output power (of only few mW) and that disappeared in short time. This behavior was attributed to thermal effects that in comparison with non-lasing regime are increased during laser emission at 1.32 μm in Nd:YAG with doping below 1.14 at.% Nd [28, 29].

The last experiments aimed laser emission at 946 nm on the quasi-three-level $^4F_{3/2} \rightarrow {}^4I_{9/2}$ transition. In this case, the HRM mirror was coated HR at $\lambda_{em}= 946$ nm and HT at the pump wavelength $\lambda_p= 807$ nm. The OCM was plane with transmission $T = 0.015$ at 946 nm. Furthermore, both mirrors were coated HT ($T > 0.95$) at the four-level 1.06 and 1.32 μm lasing wavelengths of Nd:YAG.

Laser action was obtained only under quasi-cw regime pumping. Thus, the depressed cladding waveguide DWG-5 showed lasing at 946 nm with threshold of 7.5 mJ; the maximum energy of the laser pulse was E_p = 0.12 mJ. The two-wall type waveguide WG-1 outputted pulses with energy E_p = 0.36 mJ (linearly-polarized pump beam with energy E_{pump} = 4.6 mJ), the pump energy at threshold of emission being 2.3 mJ. Although the performances were modest, these results the first on laser emission on a quasi-three-level transition in Nd-based waveguides realized by direct fs-laser writing. The use of a low-doped Nd:YAG crystal, the cooling of the laser medium, or optimization of the laser resonator and of pumping conditions could improve the laser performances at this wavelength of emission.

3. CONCLUSIONS

In conclusion, in this work we have reported on realization of two-wall type and buried depressed waveguides in 0.7-at.% Nd:YAG crystal by direct inscribing using the fs-laser technique. Laser emission on the four-level 1.06 and 1.32 wavelengths was obtained under the pump with a fiber-coupled diode laser at 807 nm. Laser pulses at 1.06 μm with 1.8 mJ energy (optical efficiency of 0.20) and cw output power of 0.54 W for 3.8 W incident pump power were measured from a 120 μm diameter buried depressed waveguide. Also, this device outputted laser pulses at 1.32 μm with 0.4 mJ energy. A two-wall waveguide yielded laser pulses at 1.06 and at 1.32 μm with 0.92 and 0.40 mJ energy, respectively. Laser action at 946 nm was observed under quasi-cw pumping. Further works will consider improvement of the writing technique and obtaining of laser emission with increased performances, as well as realization of this kind of laser waveguides in other Nd-based laser media.

Acknowledgments. This work was supported by a grant of the Romanian National Authority for Scientific Research, CNCS - UEFISCDI, project number PN-II-ID-PCE-2011-3-0363.

REFERENCES

1. C. Grivas, Progress in Quantum Electron., **35**, *6*,159–239 (2011).
2. R. V. Schmidt, I. P. Kaminov, Appl. Phys. Lett., **25**, *18*, 458–460 (1974).
3. T. Izawa, H. Nakagome, Appl. Phys. Lett., **21**, *12*, 584–586 (1972).
4. J. L. Jackel, C. E. Rice, J. J. Veselka, Appl. Phys. Lett., **41**, *7*, 607–608 (1982).
5. M. Domenech, G. V. Vázquez, E. Cantelar, G. Lifante, Appl. Phys. Lett., **83**, *20*, 4110–4112 (2003).
6. Y. Y. Ren, N. N. Dong, F. Chen, D. Jaque, Opt. Express, **19**, *6*, 5522–5527 (2011).
7. S. Nolte, M. Will, J. Burghoff, A. Tuennermann, Appl. Phys. A, **77**, *1*, 109–111 (2003).
8. A. G. Okhrimchuk, A. V. Shestakov, I. Khrushchev I, J. Mitchell, Opt. Lett., **30**, *17*, 2248–2250 (2005).

9. G. A. Torchia, A. Rodenas, A. Benayas, E. Cantelar, L. Roso, D. Jaque, Appl. Phys. Lett., **92**, *11*, 111103 (2008).
10. J. Siebenmorgen, K. Petermann, G. Huber, K. Rademaker, S. Nolte, A Tünnermann, Appl. Phys. B, **97**, *2*, 251–255 (2009).
11. T. Calmano, J. Siebenmorgen, O. Hellmig, K. Petermann, G Huber, Appl. Phys. B, **100**, *1*, 131–135 (2010).
12. Y. Tan, F. Chen, J.R. Vázquez de Aldana, G.A. Torcia, A. Benayas, D Jaque, Appl. Phys. Lett., **97**, *3*, 031119 (2010).
13. T. Tan, A. Rodenas, F. Chen, R. R. Thomson, A. K. Kar, D. Jaque, Q. Lu, Opt. Express, **18**, *24*, 24994–24999 (2010).
14. J. Siebenmorgen, T. Calmano, K. Petermann, G. Huber, Opt. Express, **18**, *15*, 16035–16041 (2010).
15. T. Calmano, A. G. Paschke, J. Siebenmorgen, S. T. Fredrich-Thornton, H. Yagi, K. Petermann, G. Huber, Appl. Phys. B, **103**, *1*, 1–4 (2011).
16. C. Zhang, N. Dong, J. Yang, F. Chen, J. R. Vázquez de Aldana, Q. Lu, Opt. Express, **19**, *3*, 12503–12508 (2011).
17. Y. Jia, N. Dong, F. Chen, J. R. Vázquez de Aldana, Sh. Akhmadaliev, S. Zhou, Opt. Express, **20**, *9*, 9763–9768 (2012).
18. D. Beckmann, D. Esser, J. Gottmann, Appl. Phys. B, **104**, *3*, 619–624 (2011).
19. N. Dong, Y. Tan, A. Benayas, J. Vázquez de Aldana, D. Jaque, C. Romero, F. Chen, Q Lu, Opt. Lett., **36**, *6*, 975–977 (2011).
20. F. Laurell, T. Calmano, S. Müller, P. Zeil, C. Canalias, G. Huber, Opt. Express, **20**, *20*, 22308–22313 (2012).
21. H. Liu, Y. Jia, J. R. Vázquez de Aldana, D. Jaque, F Chen, Opt. Express, **20**, *17*, 18620–18629 (2012).
22. Y. Ren, G. Brown, A. Ródenas, S. Beecher, F. Chen, K. Kar, Opt. Lett., **37**, *16*, 3339–3341 (2012).
23. S. Müller, T. Calmano, P. Metz, N.-O. Hansen, C. Kränkel, G. Huber, Opt. Lett., **15**, *37*, 5223–5225 (2012).
24. Y. Ren, J. R. Vázquez de Aldana, C. Feng Chen, H. Zhang, Opt. Express, **21**, *5*, 6503–6508 (2013).
25. Y. Ren, F. Chen, J. R. Vázquez de Aldana, Opt. Express, **21**, *9*, 11562–11567 (2013).
26. A. Okhrimchuk, V. Mezentsev, A. Shestakov, I. Bennion, Opt. Express, **20**, *4*, 3832–3843 (2012).
27. Y. Tan, Y. Jia, F. Chen, J.R. Vázquez de Aldana, D. Jaque, J. Opt. Soc. Am. B, **28**, *7*, 1607–1610 (2011).
28. N. Pavel, V. Lupei, T. Taira, Opt. Express, **13**, *20*, 7948–7953 (2005).
29. N. Pavel, V. Lupei, J. Saikawa, T. Taira, H. Kan, Appl. Phys. B, **82**, *4*, 599–605 (2006).